Spontaneous Immortalization of Human Epidermal Cells with Naturally Elevated Telomerase

Miguel A. Rea[1,6], Lei Zhou[2,7], Qin Qin[1], Yann Barrandon[3,8], Karen W. Easley[3], Sarah F. Gungner[4], Marjorie A. Phillips[1], William S. Holland[5], Paul H. Gumerlock[5], David M. Rocke[2] and Robert H. Rice[1]

This work explores spontaneous immortalization in keratinocytes, derived from two skin samples, that display naturally elevated telomerase activity. Serially passaged with 3T3 feeder layer support, the keratinocytes were examined for colony-forming ability, telomerase activity, telomere length, and finally gene expression using Affymetrix DNA microarrays. The cells initially exhibited normal karyotypes and low colony-forming efficiencies typical of normal epidermal cells, but after 40 passages (≈400 generations) colony-forming ability increased markedly, yielding immortalized lines exhibiting a small number of chromosomal aberrations and functionally normal p53. An improved protocol for analysis of microarray data permitted detection of 707 transcriptional changes accompanying immortalization including reduced $p16^{INK4A}$ mRNA. Telomerase activity was clearly elevated in cells even at low passage from both samples, and telomerase catalytic subunit mRNA was greatly elevated in those with elevated colony-forming ability. The data raise the possibility of an unusual natural phenotype in which aberrant telomerase regulation extends keratinocyte lifespan until rare variants evade senescence. In addition to revealing a potential tumor-prone syndrome, the findings emphasize the desirability of carefully minimizing the degree or timing of elevated expression of telomerase used to immortalize cells for therapeutic purposes.

Journal of Investigative Dermatology (2006) **126,** 2507–2515. doi:10.1038/sj.jid.5700424; published online 15 June 2006

INTRODUCTION

Since the finding that human cells in culture routinely undergo replicative senescence (Hayflick and Moorhead, 1961), considerable effort has been directed to finding the basis for this phenomenon. Many observers have noted that senescence in culture is not a reflection of replicative potential *in vivo*, suggesting that the culture environment induces damage, including through oxidative processes, mediating growth arrest (Sherr and DePinho, 2000; Rubin, 2002; Wright and Shay, 2002). A second such pathway in cultured human cells arises from the gradual shortening of telomeres in the absence of telomerase activity. Below a critical minimal length, the shortest telomeres (Hemann *et al.*, 2001; Karlseder *et al.*, 2002) activate a DNA damage checkpoint (d'Adda di Fagagna *et al.*, 2002). Although observations suggest that cells in a population can respond to either or both pathways (Itahana *et al.*, 2003; Herbig *et al.*, 2004), alternate interpretations of the data exist (Jacobs and de Lange, 2004). By whatever route, certain markers of senescence observed in culture (e.g., $p16^{INK4a}$/Arf) also accumulate in aging rodents (Krishnamurthy *et al.*, 2004).

Erosion of telomeres to a critical length, preventing further growth, is envisioned to provide a block to neoplasia. In the absence of such a block, continued cycling is associated with chromosomal instability (Chan and Blackburn, 2004). Resulting chromosomal rearrangements are expected to be lethal to most of the cells in which they occur, but rare variants with neoplastic potential can arise. Thus, as seen in aging telomerase-deficient mice, chromosomal instability from a lack of telomeres can drive the appearance of spontaneous malignancies (Rudolph *et al.*, 1999). The incidence of non-reciprocal chromosomal translocations and early neoplastic lesions in certain tissues is dramatically increased in such mice that harbor additional checkpoint defects (Maser and DePinho, 2002). However, as the malignant cells that evolve need chromosome stability to grow well, telomerase deficiency can lead to a reduction in ultimate yield of advanced tumors (Rudolph *et al.*, 2001). These findings are consistent with observations that human tumor cells have short

[1]*Department of Environmental Toxicology, University of California, Davis, California, USA;* [2]*Division of Biostatistics, University of California, Davis, California, USA;* [3]*Department of Cell Biology, Harvard Medical School, Boston, Massachusetts, USA;* [4]*Sutter Memorial Hospital, Sacramento, California, USA and* [5]*Division of Hematology and Oncology, Department of Internal Medicine, University of California Davis Cancer Center, Sacramento, California, USA*

[6]*Current address: Facultad de Química, Universidad Autónoma de Querétaro, Cerro de las Campanas s/n, Querétaro, Qro. 76010, México.*

[7]*Current address: Amgen, Thousand Oaks, California 91320-1799, USA.*

[8]*Current address: Laboratory of Stem Cell Dynamics, Swiss Federal Institute of Technology, Lausanne, Switzerland.*

Correspondence: Dr Robert H. Rice, Department of Environmental Toxicology, University of California, Davis, California 95616-8588, USA. E-mail: rhrice@ucdavis.edu

Abbreviations: CGH, comparative genomic hybridization; CFE, colony-forming efficiency; TERT, telomerase catalytic subunit

Received 16 July 2005; revised 24 April 2006; accepted 28 April 2006; published online 15 June 2006

telomeres (van Heek *et al.*, 2002) but have reactivated telomerase expression in the large majority of cases (Kim *et al.*, 1994). The importance of telomerase activity for tumor survival has raised its profile as a potential target for chemotherapy with enzyme inhibitors or other treatments reducing telomerase activity (Morin, 1995; Li *et al.*, 2005).

In contrast, the potential of telomerase to extend the lifespan of cells *in vivo* has suggested its application to regenerative therapy (Shay and Wright, 2000). Recent applications show advantages of its introduction by a retroviral vector into human endothelial cells that are then functional in mice (Yang *et al.*, 2001), and into human bone marrow stem cells to enhance their osteogenic potential *in vivo* (Shi *et al.*, 2002; Simonsen *et al.*, 2002). Telomerase overexpression itself has not been found to induce neoplastic changes in cultured recipient cells such as fibroblasts (Morales *et al.*, 1999), but general overexpression in transgenic mice has been found to promote mammary carcinogenesis (Artandi *et al.*, 2002), and overexpression in the epidermis increases the sensitivity of the skin to chemical carcinogens (Gonzalez-Suarez *et al.*, 2001), raising concern about long-term consequences of this therapeutic approach. Observation that a sample of human epidermal cells displaying naturally elevated levels of telomerase activity became spontaneously immortalized (Rice *et al.*, 1993; Rea and Rice, 2001) has prompted the present investigation. Immortalization of cells from the original and a second, independently derived, skin sample has been analyzed in more detail as examples of a rare phenotype in the human population.

RESULTS

Epidermal cells from the same skin sample that gave rise to the original SIK line of spontaneously immortalized keratinocytes (Rice *et al.*, 1993) were serially propagated starting with cells frozen in liquid nitrogen at passage 3. The cells initially exhibited low colony-forming efficiency (CFE) values, similar to those from normal epidermal cells (Figure 1a). After attaining maximal values of ≈10%, the CFE declined starting at passage 20 and reached minimal values of 0.5–1% by passage 40. At passage 30, the cells were split into two parallel lineages (SIKer, SIKly) that were indistinguishable until passage ≈45, at which point the CFE values diverged. The SIKer line exhibited increasing CFE until it reached a plateau at ≈35% by passage 60. In contrast, the SIKly line increased in CFE to ≈5%, a level maintained through passage 70.

Derived from an independent tissue sample, the HFS2 line also exhibited increasing CFE with passage (Figure 1b, lower curve). The CFE was 2–3% at passages 6 and 8, slightly higher (5%) at passage 37, and ≈22% by passage 61. The fraction of normal human epidermal cells capable of forming progressively growing colonies is known to decline substantially if cultures are harvested when individual colonies are large or merge at confluence (Barrandon and Green, 1987). The method of measuring CFE near confluence in this study readily revealed the increases noted at later passages. By contrast, when CFE measurements were performed using

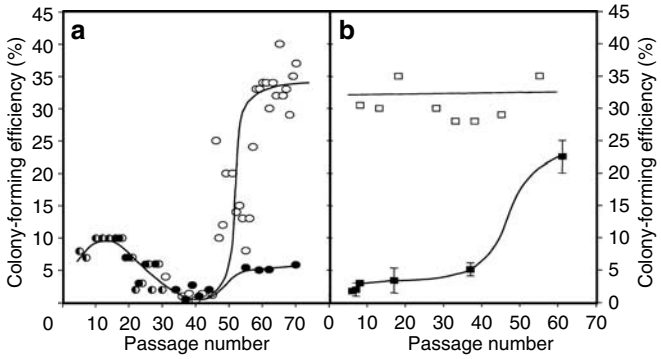

Figure 1. Colony-forming efficiency *versus* passage number. (**a**) Values of SIKer (open circles) and SIKly (filled circles) cultures were assayed under the usual conditions near confluence. The two sublineages were separated from a common lineage (half-filled circles) at passage 30. (**b**) Values for HFS2 cultures were measured near confluence (filled boxes) or while colonies were in early log phase growth (open boxes).

cultures well before confluence, where colonies were small enough that the ability to form progressively growing colonies upon subculture is maintained (Barrandon and Green, 1987), the CFE was uniformly high, nearly 30% or more throughout the passages examined (Figure 1b, upper curve). This contrast emphasizes that the rate at which HFS2 germinative cells left the mitotic pool as colony size increased was reduced at higher passage. Thus passaging of the cells when they were near confluence rather than while the colonies were still small likely sped the takeover of variants with elevated CFE.

As established cell lines generally exhibit chromosomal aberrations, karyotypes of the present lines were examined. As illustrated in Figure 2a, standard Giemsa banding showed that by passage 72 the SIKer line had acquired an extra isochromosome 1q and an extra chromosome 20 and had lost one chromosome 19. Three additional marker chromosomal fragments were also observed whose origin was not possible to determine by standard Giemsa staining. Similarly, the HFS2 line showed a normal karyotype (46,XY) at passage 9, but it had acquired a derivative chromosome 6 containing a translocation from chromosome 18 and suffered the loss of one chromosome 18 by passage 20 (45,XY,der (6)t(6;18)(q12;q11.2),−18). In a small proportion of the cells, loss of the remaining chromosome 18 and/or acquisition of an extra chromosome 21 were also noted at this passage. At passages 40 and 60 (shown in Figure 2b), HFS2 cells had the same karyotype as in passage 20, although losses of chromosomes 9, 13, or 21 were observed in a small fraction of the cells. The more discriminating method of comparative genomic hybridization (CGH) was employed to examine the chromosomal complement of the SIKly line and showed that the cells of passage 67 contained a duplication of chromosome 1q (Figure 2c, top panel). The presence of the 1q aberration in the SIKer line suggests that it was already present when the cells were divided into the two sublines at passage 30. This technique did not reveal aberrations in passage 7 cells from the HFS2 tissue sample (Figure 2c,

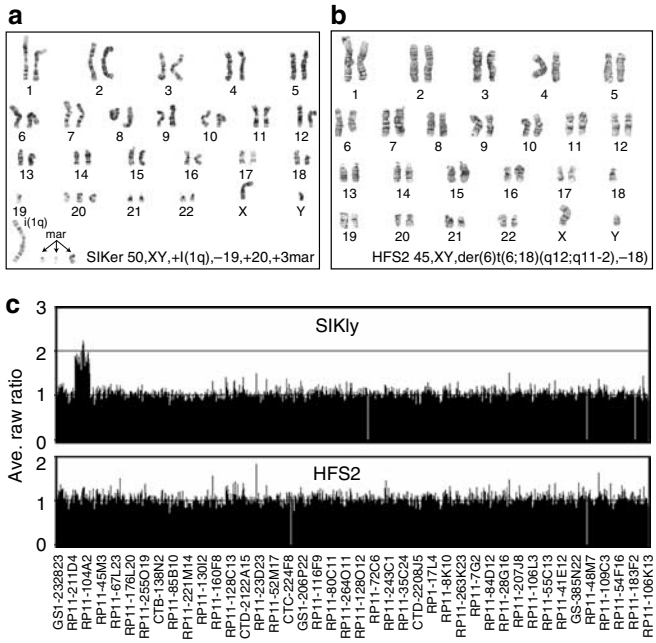

Figure 2. Chromosomal complement of spontaneously immortalized lines. (**a**) Passage 72 SIKer and (**b**) passage 40 HFS2 cells were examined by G-banding, revealing (**a**) three marker chromosomes or (**b**) an aberrant chromosome 6. (**c**) Passage 67 SIKly and passage 7 HFS2 cellswere examined by CGH showing the relative hybridization signal over the clones representing the human genome (clone identities given in the *X*-axis). The elevated signal in the SIKly cells represents a doubling of genetic material in chromosome 1q.

bottom panel) or passage 3 cells from the sample from which the SIK lines were derived (not shown), both consistent with the normal karyotype observed by chromosomal banding (Rice *et al.*, 1993). This negative result was confirmed with SIK (passage 6) and HFS2 (passage 5) cultures using Agilent Human Genome 44B CGH array chips. The unusual immortalization by these cells may well arise from DNA damage, but if so it appears to be small scale (e.g., point mutation or small insertion/deletion).

Telomerase activities in the lines were examined under conditions of optimal growth (Table 1). As reported previously (Rea *et al.*, 1998; Rea and Rice, 2001), the activities in SIK cultures were higher than in normal epidermal cultures and increased at higher passages. Present experiments revealed that the activity was 4-fold and 7-fold higher than normal at passages 6 and 42, respectively. The activity in the SIK and SIKer lines (passage 52) was comparable, whereas the activity of the SIKly line (passage 52) was essentially the same as that of passage 6. Telomerase activity in the HFS2 line at passage 6 was twice that in the normal cultures (hEp6) and more than 3-fold the level in hEp6 by passage 61. As shown in Table 1 and by sampling of several other passages (not shown), the telomerase activity did not increase monotonically with increasing passage whereas CFE declined, but it was substantially higher when immortalization became evident by high CFE. Present experiments in cultures grown in the presence or absence of EGF also showed that telomerase activity was markedly higher in cultures with a higher growth rate, consistent with findings of others and as previously shown (Rea and Rice, 2001).

Table 1. Relative levels of TERT mRNA and telomerase activity[1]

Cell line	TERT mRNA	Telomerase
hEp6	1	1
SIK6	24[2]	4[2]
SIK23	22[2]	2.1[2]
SIK42	124[2]	7.3[2]
SIKer52	105[2]	6.5[2]
SIKly52	16[2]	3.3[2]
HFS6	1.3	2.1[2]
HFS26	4.9	1.3
HFS61	67[2]	3.4[2]

[1]Relative levels of TERT mRNA and telomerase activity in three (TERT) or four (telomerase) real-time PCR experiments.
[2]Significantly different from hEp6, arbitrarily taken as 1, by analysis of variance ($P<0.001$).

Telomerase catalytic subunit (TERT) mRNA levels were undetectable by real-time PCR analysis a week after confluence in SIK cultures (passage 6), paralleling measurements of catalytic activity as a function of days after inoculation (Rea and Rice, 2001). Measured well before confluence, the SIK lineage exhibited 20-fold higher TERT mRNA levels than normal epidermal cells at passages 6 and 23, whereas at higher passages (42 and 52, respectively), the SIK and SIKer lines had >100-fold the normal level of TERT mRNA (Table 1). By contrast, the level in the SIKly line was comparable to the low-passage SIK cultures. Also in contrast, the HFS2 line did not display elevated TERT mRNA at the low passages (where CFE was not elevated), but the level was ≈50-fold normal (hEp6) in passage 61 cells that displayed an order of magnitude increase in CFE. In each case of elevated mRNA, the levels were much lower in cultures grown without EGF (not shown), similar to the differences noted in telomerase activity (Rea *et al.*, 1998; Rea and Rice, 2001).

Telomere restriction fragment (TRF) lengths in the cell lines, measured as a function of passage, are given in Figure 3. The HFS2 line had the longest telomeres (~6 kb) among those examined, and their length was essentially constant through >60 passages (>500 generations). By contrast, TRFs in the SIKer line were nearly as long initially but gradually declined to 3 kb by passage 50, a phenomenon now noted for the original SIK line and shown for comparison. In both SIK and SIKer lines, no further declines were noted after passage 50, at which point telomere lengths appeared to increase. The SIKly line, which was separated from SIKer at passage 30, exhibited TRF lengths of 2 kb by passage 50 but did not appear to increase either in telomere length or in colony-forming efficiency beyond that point. The cells continued to grow well without the usual signs of impending sensescence (e.g., replacement of small cells by squames throughout the colonies, lack of progressive growth by most colonies).

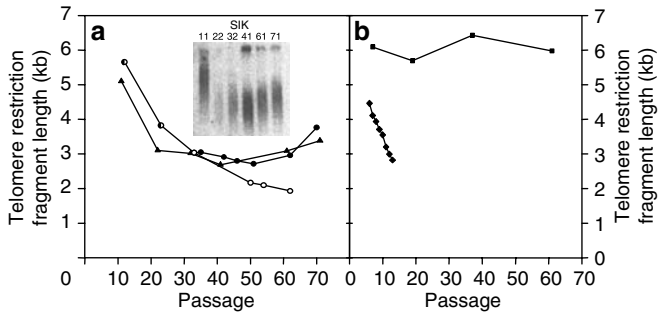

Figure 3. Telomere restriction fragment length *versus* passage. Plotted are weighted averages obtained from analyses of DNA samples from mass cultures taken at the indicated passages on the horizontal axis. (**a**) Values for SIK (triangles), SIKer (filled circles), SIKly (open circles), and the lineage giving rise to SIKer and SIKly (half-filled circles). The inset is a representative gel result showing the relative migration of digested DNA from the SIK line at the indicated passages above the lanes (sizes determined from *Hin*dIII fragments of lambda DNA, not shown). (b) Values for hEp (diamonds), which senesced at passage 15, and HFS2 (squares).

To obtain a better understanding of the immortalization process and the properties of cells with high CFE, transcriptional profiles were obtained by DNA microarray (Affymetrix U95Av2 chips). For this purpose, two samples (taken as replicates) each of the SIKer (passages 49 and 73) and SIKly (passages 57 and 64) lines were examined when near-maximal CFE was attained (passages >48) and compared to two samples of the cells (passages 3 and 12) before the immortalization process became evident. In parallel, two samples of the original immortalized SIK line (passages 34 and 45) with high CFE were also examined. After statistical treatment, a total of 707 genes were obtained where the transcription was significantly altered ($P=0.05$) between at least one of the immortalized lines compared to passage 3 and 12 cells (see Table S1 for complete list). Among these, Table 2 gives the most dramatic transcriptional changes exhibited in common by the SIK, SIKer and SIKly lines. Of the 17 transcripts selected on this basis, five were also examined by real-time PCR. In all cases, the changes revealed by the

Table 2. Transcriptional changes shared by SIK, SIKer, and SIKly lines[1]

Affymetrix probe	Gene name	Intensity[2] (low passage)	FC-SIK[3]		FC-SIKly[3]		FC-SIKer[3]		FC-HFS2[4]	HFS2/Low[5]
			Affy[6]	PCR[7]	Affy[6]	PCR[7]	Affy[6]	PCR[7]	PCR	PCR
Suppressed										
38608_at	LGALS7	712	ND[8]	—	ND[8]	—	ND[8]	—	—	—
38326_at	G0S2	116	ND[8]	0.004	ND[8]	$<10^{-6}$[8]	ND[8]	$<10^{-6}$[8]	$<10^{-6}$[8]	0.7
39698_at	HOP	285	0.25	0.03	0.9	0.07	0.3	0.12	0.11	0.53
40567_at	TUBA3	221	0.14	—	0.31	—	0.17	—	—	—
37754_at	LGALS3BP	1,012	0.2	—	0.25	—	0.22	—	—	—
38440_s_at	FLJ20811	197	0.14	—	0.1	—	0.1	—	—	—
851_s_at	IRS1	218	0.18	0.14	0.24	0.17	0.4	0.4	1.9	0.12
36057_at	ALEX2	51	ND[8]	<0.001[8]	ND[8]	<0.001[8]	ND[8]	<0.001[8]	<0.001[8]	0.19
39528_at	RRAD	412	0.30	—	ND[8]	—	0.09	—	—	—
1713_s_at	CDKN2A	105	0.21	0.26	0.09	0.10	0.39	0.18	1.5	0.29
Stimulated										
33792_at	PSCA	68	2.5	—	8.7	—	6.9	—	—	—
33143_s_at	SLC16A3	380	2	—	4.2	—	4.4	—	—	—
33679_f_at	TUBB2	1,303	2	—	1.7	—	2	—	—	—
757_at	ANXA2	539	2.7	—	3.9	—	3.8	—	—	—
38131_at	PTGES	329	3.1	—	2.9	—	3.3	—	—	—
37043_at	ID3	975	2.7	2.7	1.6	1.7	2.1	2.1	5.1	0.3
34703_f_at	HHLA1	38	13	—	31	—	16	—	—	—
34702_f_at	psiTPTE22	2.6	175	—	495	—	257	—	—	—

[1]Using the processed microarray data for significantly altered transcripts, probes were selected in which the changes were in the same direction for SIK, SIKly, and SIKer lines, each change was ⩾1.5 (increase or decrease), and the sum of the three changes was >6. CDKN2A ($p16^{INK4a}$) is also included.
[2]Average of SIK passages 3 and 12 (low passages) in Affymetrix units (MAS4.0).
[3]Fold change (ratio of values at high to low passage) for the indicated lines.
[4]Fold change (ratio of values) of HFS2 passage 61 to passage 5.
[5]Fold change (ratio of values) of HFS2 passage 5 to SIK passage 6.
[6]Average intensities of passages 34 and 45 (SIK), 57 and 64 (SIKly), or 49 and 73 (SIKer) divided by the average intensity for passages 3 and 12.
[7]Ratio of amounts of the indicated mRNAs (normalized to 18S) for passages 41 (SIK), 71 (SIKly), or 70 (SIKer) to SIK passage 6.
[8]Below the limit of detection.

two methods were in the same direction. The quantitative matches were especially good for G0/G1 switch gene 2 (G0S2), insulin receptor substrate 1 (IRS1), armadillo protein lost in epithelial cancers 2 (ALEX2) and inhibitor of DNA binding 3 (ID3). Real-time PCR also indicated that substantial changes in transcription of G0S2, HOP, ALEX2 and ID3 were parallel in the HFS2 line to those in SIK, SIKer and SIKly during immortalization. Only the change in IRS1 transcription was in the opposite direction.

DNA microarray and real-time PCR revealed that transcription of p16 (CDKN2A), also among the significant changes, was considerably reduced in the SIK, SIKer and SIKly lines to less than half that before immortalization (Table 2). (The p19Arf transcript (probe 1797_at) had a low intensity (48 MAS4.0 units) that was increased 11, 90, and 2% in high-passage SIK, SIKer and SIKly array samples, respectively.) In the HFS2 line, however, p16 transcription was not suppressed but actually increased slightly ($\approx$50%), although the cells of passage 5 exhibited only $\approx$30% the mRNA level of passage 6 SIK cultures. Of considerable potential functional significance, this observation prompted estimation of the protein level by immunoblotting. As shown in Figure 4, the relative amounts of p16 were comparable to those in normal epidermal cells with the exception of the negative control, the SCC9 carcinoma line deficient in p16 expression. Expression of p16 protein did not change much in HFS2 from passages 5 through 61 and was comparable to that in SIK passage 6 cultures (not shown). The p16 coding region was sequenced using genomic DNA from SIK (passage 41), SIKer (passage 70), SIKly (passage 71), and HFS2 (passage 61), and only the native sequence was observed. The methylation status of the p16 promoter was examined from SIK (passages 5 and 41), SIKer (passage 71), and SIKly (passage 69), but repeated measurements revealed little or no methylation, indicating that expression was not diminished through methylation of CpG islands (Huschtscha and Reddel, 1999).

DISCUSSION

Current models of the evolution of common human neoplasms such as breast cancer (Chin *et al.*, 2004) have genomic instability, leading to chromosomal aberrations, participating in their early development. The aberrations likely arise as a result of telomere erosion in benign lesions, generating cells with malignant characteristics. The latter have a need for chromosomal stability for survival and vigorous growth, providing a selection for telomerase reactivation. Occurring early in the generation of a neoplastic lesion, DNA damage that removes checkpoints to unrestrained growth could lead to telomere erosion, thus precipitating instability. From this perspective, high-level telomerase activity in cells would prevent instability induced by telomere erosion and, by increasing their lifespan, permit accumulation of damage to other checkpoint guardians. Although the p53 tumor suppressor gene is a common target in the epidermis leading to neoplasia (Grossman and Leffell, 1997), its inactivation is not required for immortalization (Kiyono *et al.*, 1998; Allen-Hoffmann *et al.*, 2000). In the present case, Western blotting (data not shown) indicated that the lines all expressed p53, and its ability to stimulate transcription in yeast strain yIG397 (Flaman *et al.*, 1995) appeared normal (Table S2).

Numerous investigators have found that high levels of telomerase alone are insufficient to induce immortalization and provide examples in keratinocytes and mammary epithelial cells (and other cell types) where inactivation or disappearance of $p16^{INK4a}$ accompanies immortalization (Romanov *et al.*, 2001; Rheinwald *et al.*, 2002). Although $p16^{INK4a}$ mRNA levels were markedly reduced, the protein was neither absent nor mutated in the present experiments. Substantial levels of the protein were evident, comparable to those seen in normal, even senescent, human epidermal cells. The importance of $p16^{INK4a}$ loss in permitting escape from senescence has been well demonstrated with or without a 3T3 feeder layer (Rheinwald *et al.*, 2002). We speculate that the present lines have developed an insensitivity to p16 somewhere in its signaling pathway, although the possibility that escape may occur by other routes must be considered. Present observations with the SIK and HFS2 lines fit a model where, unlike in cultures harboring expression vectors designed to produce very high telomerase levels, the elevation is sufficient to confer a lengthened lifespan but not high enough to prevent eventual telomere shortening. The original observation of immortalization by the SIK line did not reveal a slow growth phase (Rice *et al.*, 1993), but the present derivation of SIKer and SIKly lines occurred during a long period of decreasing colony-forming ability. The resulting immortalized SIK and SIKer lines had a small number of chromosomal aberrations, some of which likely occurred as a result of telomere erosion.

In this work, large transcriptional changes among known oncogenes or tumor suppressor genes were not observed. Identifying novel senescence escape routes is not straightforward, especially if the concerted action of small changes among several genes is involved, but surveying transcriptional changes in cells undergoing immortalization by DNA microarray may help find pathways that are altered and permit escape. In the present case, loss of ALEX2, a potential tumor suppressor (Kurochkin *et al.*, 2001), and IRS1, inactivation of the homolog of which in *Drosophila. melanogaster* confers longevity (Clancy *et al.*, 2001), provide starting points for further investigation. Despite exhibiting common transcriptional changes, some of which likely

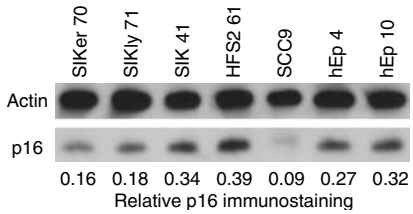

Figure 4. Immunoblotting of p16. Samples of the indicated cells and passage number were solubilized in SDS-dithiothreitol and examined by immunoblotting. The relative amount of p16 compared to β-actin is given below the appropriate lane. The hEp10 culture was senescent and was harvested a week after growth had stopped.

contribute to immortalization, clear differences in properties were evident among the lines. Nevertheless, examination of the compendium of transcriptional changes (Table S1) provides clues to the improved growth of the SIKer and SIKly lines. For example, important members of the mitogen-activated protein kinase cascade were seen to be elevated including the EGF receptor, the Shc adaptor, c-Raf, MAPK/ERK kinase 1/2 and ERK1/2. This constellation of changes could sensitize the cells to growth factor stimulation, including paracrine stimulation through tumor growth factor-α secretion.

The presence of naturally elevated telomerase in human epidermal cells could be a rare phenotype in the population of particular concern if telomerase can promote cancer-proliferative properties as recently proposed (Li *et al.*, 2005). A recent report that TERT is expressed at a low level in S phase in cultured normal human fibroblasts (Masutomi *et al.*, 2004), thought to lack expression, suggests that its upregulation may be easier than previously believed. Stimulation by perturbing the cellular microenvironment, including by growth factors such as EGF in SIK lineages or even environmental chemicals such as 2,3,7,8-tetrachlorodibenzo-*p*-dioxin (Ray and Swanson, 2004) in HFS2 cells (Rea and Rice, 2000), could prolong the period before growth arrest and lead eventually to acquisition of neoplastic properties. Efforts to show in the present lines altered levels of TERT regulators such as the PinX1 protein (Banik and Counter, 2004) by Northern blotting or Mad1 and Menin (Lin and Elledge, 2003) by immunoblotting have been unsuccessful. Transcriptional regulation of TERT in general is important, including possible release of repressor activity (Racek *et al.*, 2005), and is evident in these cells. Present results indicate that post-transcriptional regulation is also important inasmuch as measured increases in activity occur to a lower extent than those of mRNA. These cells may provide useful subjects for exploration of translational or post-translational effects.

MATERIALS AND METHODS

Cell culture

Keratinocytes were cultured with 3T3 feeder layer support (Rheinwald and Green, 1975) in a 3:1 mixture of Dulbecco Vogt Eagle's and Ham's F-12 media supplemented with 5% fetal bovine serum, 0.4 μg/ml hydrocortisone, 5 μg/ml insulin, 5 μg/ml transferrin, 20 pM T_3, 0.18 mM adenine, 10 ng/ml EGF and 10 ng/ml cholera toxin (Allen-Hoffmann and Rheinwald, 1984). Two new lines (SIKer and SIKly) were derived from the same tissue sample as SIK (ostensibly normal newborn circumcision skin) starting with an ampule frozen in liquid nitrogen at passage 3, where the cells had a normal karyotype (Rice *et al.*, 1993). At passage 30, the lineage was divided into two separate strains that developed into distinct lines. The HFS2 line was derived from human fetal sole skin (22 weeks of gestation). For the present characterization, trypsinized cultures at an estimated 75% confluence were used for the various parameters measured. CFE values were measured as the percentages of inoculated cells that gave rise to macroscopic colonies (>50 cells) after 10–14 days; dishes were inoculated so as to yield ≈50 colonies. Ordinarily, cultures were passaged as they approached (estimated 1 day before) confluence and diluted (judging by the CFE of the previous passage) to give ≈10,000 colonies per culture. Despite having comparable numbers of colonies, the cultures gradually slowed in growth rate, being subcultured roughly at weekly intervals at low passage and at 2–3 weeks intervals after passage 30 until rises in CFE and growth rate ultimately occurred together. The SIKer, SIKly, and HFS2 lines (Figure S1) were as dependent upon EGF for growth as normal epidermal cells, as previously found for SIK (Rice *et al.*, 1993). Short tandem repeat analysis revealed the same pattern in SIKer and SIKly lines as in the original SIK line, whereas passages of the HFS2 line gave a distinct pattern (Figure S2). Skin samples (otherwise discarded) were obtained and experiments were performed with institutional approval.

Chromosomal analysis

For G-banding, logarithmically growing cells were arrested in metaphase using colcemid (50 ng/ml), trypsinized, incubated for 30 minutes in 75 mM KCl, fixed in methanol:acetic acid (3:1) and dropped onto cold glass slides. After aging for several days, the slides were treated briefly with trypsin and stained with Giemsa. A minimum of 10 well spread metaphases from G banded cultures were examined to obtain the characteristic patterns illustrated. Chromosomes were identified with assistance from computer software. For CGH, randomly primed fluorescent probes made from cell DNA were hybridized with reference genomic DNA providing about 1.4 Mb resolution across the human genome (Kraus *et al.*, 2003). SIK passage 6 and HFS2 passage 5 cells were also examined for deletions or duplications using Agilent Human Genome CGH Microarray 44B chips containing 43,000 60-mer oligonucleotide probes covering exon and intron sequences (average spatial resolution of 35 kb).

p16 analysis

Exons of $p16^{INK4a}$ were amplified from genomic DNA by PCR using primers as described (Hussussian *et al.*, 1994; Florl *et al.*, 2000), and the sequences were determined by DNA Sequencing Facility of the University of California, Davis. Immunoblotting of p16 and β-actin were performed using antiserum clones G175-405 (BD Pharmingen Inc., San Diego, CA) and AC-74 (Sigma Chemical Company, St Louis, MO), respectively, and developed with ECL Plus reagent (GE Healthcare Bio-Sciences Corp., Piscataway, NJ). Amounts of p16 protein relative to β-actin from confluent cultures were estimated from the scanned films using ImageQuant software. Promoter methylation status was examined using the CpGenome DNA Modification Kit from Chemicon International (Temecula, CA).

DNA isolation

For CGH, trypsinized cells were digested overnight with proteinase K in the presence of SDS, and the DNA was precipitated with ethanol and dissolved in water. For telomere length analysis, keratinocyte cultures were rinsed twice in isotonic neutral buffered saline and lysed in 0.1% SDS – 0.1 M EDTA – 0.05 M Tris-HCl (pH 8). The lysate was digested first with DNAse-free bovine pancreatic ribonuclease A (10 μg/ml) for 1 hour at 37°C, then with proteinase K (100 μg/ml) for 5 hours at 60°C and finally was extracted with phenol–chloroform. The DNA was precipitated with ethanol, redissolved in TE buffer, and the concentration estimated spectrophotometrically.

Terminal restriction fragment length

Genomic DNA (10 μg) was restricted with *Hin*fI and *Rsa*I (50 U each) for 24 hours at 37°C. After phenol–chloroform extraction and ethanol precipitation, the restriction fragments were separated in a 0.6% agarose gel (in parallel with *Hin*dIII fragments of lambda DNA for size estimation) and blotted to a nylon membrane. The membrane was prehybridized for 1 hour and then hybridized for 5 hours at 65°C in 10 × Denhardt's solution – 10 × SSC – 2 mM Na_2HPO_4 – 0.08 mM sodium pyrophosphate containing 10^6 c.p.m./ml of a ^{32}P end-labeled 41-base telomere probe, $(CCCTAA)_6CCCTA$. The washed blot was quantitated by phosphorimaging. The image for each DNA sample (a smear) was divided into a grid of 10–20 lengthwise segments, where background values were calculated from the top and bottom segments and subtracted from the central segments. The mean TRF length (L) was the weighted average of the signal (S_i) of each segment of each length (L_i) summed over the i intervals: $L = \sum S_i L_i / \sum S_i$.

Telomerase assay

Initially, the telomerase repeat amplification protocol was employed (Piatyszek *et al.*, 1995; Rea *et al.*, 1998) with extracts of 10^5 trypsinized cells, analysis in 10% non-denaturing polyacrylamide gels and quantitation by phosphorimaging (Rea *et al.*, 1998). Similar results, but with much greater sensitivity (2,000 trypsinized cells), were obtained using a SYBR® green (Applied Biosystems, Foster City, CA) real-time PCR method (Wege *et al.*, 2003). Initial measurements in the range of 400–2,000 cells, counted using a Beckman-Coulter Multisizer 3 (Invitrogen, Carlsbad, CA), indicated that the upper number was best for detecting the low activity displayed by the normal cells (mean C_t value 35.17). The lingual squamous carcinoma line SCC9 (Rheinwald and Beckett, 1981), used as a positive control, exhibited 21-fold higher telomerase activity than the highest epidermal keratinocytes examined (SIK42).

Real-time PCR measurements of relative mRNA levels

Newly confluent or, in the case of telomerase reverse transcriptase (hTERT) mRNA, half confluent cultures were dissolved in Trizol reagent (Invitrogen), and total RNA was reverse transcribed with the high-capacity cDNA Archive Kit (Applied Biosystems). The relative amounts of p16, β-actin and other cDNAs were quantitated using Assay on Demand kits (Applied Biosystems) with ABI 7300 and 7700 Sequence Detection Systems, each sample being analyzed in triplicate. For confirmation of mRNA levels corresponding to DNA microarray results, C_t values for p16 cDNA ranged from 21.38 to 24.98, and those for β-actin ranged from 16.33 to 17.56. In measurements of relative hTERT mRNA, SCC9 levels (positive control) were 22-fold higher than those in SIK42 (mean C_t value for the latter of 28.96). Relative hTERT mRNA levels were calculated after normalizing for β-actin mRNA in each cell sample. Statistical significance for telomerase activity and TERT mRNA (Table 1) was analyzed from the log cycle times (as is customary) using an analysis of variance model incorporating the cell line and the experiment (to adjust for experiment-to-experiment variation). Tukey's honest significant difference test for *post hoc* comparisons indicated that all the cell lines had significantly greater expression of TERT mRNA than hEp6 except for HFS6 and HFS26, which were not significantly different, whereas the telomerase activities were significantly different from hEp6 except for HFS26. These findings are summarized in box plots of log(cycle time), adjusted for experiment, in Figure S3.

Expression profiling and analysis

Newly confluent cultures were harvested in Trizol reagent (Invitrogen) and double-stranded cDNA was synthesized using total RNA (10 μg/sample) and the SuperScript Choice system (Invitrogen) with oligo $(dT)_{24}$ priming. ComplementaryRNA was transcribed with T7 RNA polymerase and biotin-labeled nucleotides, purified with RNeasy spin columns (Qiagen, Valencia, CA), fragmented, hybridized overnight with U95Av2 arrays (Affymetrix, Santa Clara, CA) and detected using streptavidin-labeled phycoerythrin as described previously (Rea *et al.*, 2003). Statistical analysis of the data is described in an appendix (see Supplementary Method) giving a protocol for the analysis of gene expression data, especially from Affymetrix GeneChips. This protocol involves background correction, data transformation, chip normalization, and probe summary construction. Then, for each gene, a statistical analysis is conducted with improved power using an empirical Bayes method, and the significance is evaluated using a false discovery rate method. Particular differences contributing to the significance of the analysis of variance F-statistics are calculated, showing which genes are significantly different for which pairwise comparisons. This protocol is quite general and can be adapted to the analysis of any expression array experiment having sufficient biological replication to give non-zero degrees of freedom for error (seemingly an irreducible requirement for a minimally informative experiment). Software to implement these methods is available from D.M. Rocke (dmrocke@ucdavis.edu) in the form of code for the R statistical system (Ihaka and Gentleman, 1996).

CONFLICT OF INTEREST

The authors state no conflict of interest.

ACKNOWLEDGMENTS

We thank Dr Jeff P. Gregg for facilitating the Affymetrix microarray analyses and performing Agilent CGH microarrays, Drs Rick Seagraves and Daniel Pinkel for performing initial CGH analyses, David Kiewlich for Bad-1 and Menin immunoblotting, Dr Kayoko Nishi-Schnier for PinXi northern blots, and Dr Howard Green for his encouragement. This research was supported by USPHS Grants AR27130, ES05705, ES04699, and AG15404, CONACYT agreement 92991, and the Universidad Autónoma de Querétaro.

SUPPLEMENTARY MATERIAL

Figure S1. EGF dependence.

Figure S2. Short tandem repeat analysis.

Figure S3. Statistical analysis of TERT mRNA and telomerase measurements.

Table S1. Transcripts with significant changes.

Table S2. Yeast p53 functional assay.

Supplementary Method. Statistical protocol for expression array analysis.

REFERENCES

Allen-Hoffmann BL, Rheinwald JG (1984) Polycyclic aromatic hydrocarbon mutagenesis of human epidermal keratinocytes in culture. *Proc Natl Acad Sci USA* 81:7802–6

Allen-Hoffmann BL, Schlosser SJ, Ivarie CA, Sattler CA, Meisner LF, O'Connor SL (2000) Normal growth and differentiation in a spontaneously immortalized near-diploid human keratinocyte cell line, NIKS. *J Invest Dermatol* 114:444–55

Artandi SE, Alson S, Tietze MK, Sharpless NE, Ye S, Greenberg RA *et al.* (2002) Constitutive telomerase expression promotes mammary carcinomas in aging mice. *Proc Natl Acad Sci USA* 99:8191–6

Banik SSR, Counter CM (2004) Characterization of interactions between PinX1 and human telomerase subunits hTERT and hTR. *J Biol Chem* 279: 51745–8

Barrandon Y, Green H (1987) Three clonal types of keratinocyte with different capacities for multiplication. *Proc Natl Acad Sci USA* 84: 2302–6

Chan SRWL, Blackburn EH (2004) Telomeres and telomerase. *Philos Trans R Soc London B* 359:109–21

Chin K, Ortiz de Solorzano C, Knowles D, Jones A, Chou W, Rodriguez EG *et al.* (2004) *In situ* analyses of genomic instability in breast cancer. *Nat Genet* 36:984–8

Clancy DJ, Gems D, Harshman LG, Oldham S, Stocker H, Hafen E *et al.* (2001) Extension of life-span by loss of CHICO, a *Drosophila* insulin receptor substrate protein. *Science* 292:104–6

d'Adda di Fagagna F, Reaper PM, Clay-Ferrace L *et al.* (2002) A DNA damage checkpoint response in telomere-initiated senescence. *Nature* 426:194–8

Flaman JM, Frebourg T, Moreau V, Charbonnier F, Martin C, Chappuis P *et al.* (1995) A simple p53 functional assay for screening cell lines, blood and tumors. *Proc Natl Acad Sci USA* 92:3963–7

Florl AR, Franke KH, Niederacher D, Gerharz CD, Seifert HH, Schulz WA (2000) DNA methylation and the mechanisms of CDKN2A inactivation in transitional cell carcinoma of the urinary bladder. *Lab Invest* 80: 1513–22

Gonzalez-Suarez EES, Ramirez A, Flores JM, Martin-Caballero J, Jorcano JL, Blasco MA (2001) Increased epidermal tumors and increased skin wound healing in transgenic mice overexpressing the catalytic subunit of telomerase, mTERT, in basal keratinocytes. *EMBO J* 20:2619–30

Grossman D, Leffell DJ (1997) The molecular basis of nonmelanoma skin cancer. New understanding. *Arch Dermatol* 133:1263–70

Hayflick L, Moorhead PS (1961) The serial cultivation of human diploid cell strains. *Exp Cell Res* 25:585–621

Hemann MT, Strong MA, Hao L-Y, Greider CW (2001) The shortest telomere, not average telomere length, is critical for cell viability and chromosome stability. *Cell* 107:67–77

Herbig U, Jobling WA, Chen BPC, Chen DJ, Sedivy JM (2004) Telomere shortening triggers senescence of human cells through pathway involving ATM, p53, and $p21^{CIP1}$, but not $p16^{INK4a}$. *Mol Cell* 14:501–13

Huschtscha LI, Reddel RR (1999) $p16^{INK4a}$ and the control of cellular proliferative life span. *Carcinogenesis* 20:921–6

Hussussian CJ, Struewing JP, Goldstein AM, Higgins PA, Ally DS, Sheahan MD *et al.* (1994) Germline p16 mutations in familial melanoma. *Nat Genet* 8:15–21

Ihaka R, Gentleman R (1996) R: a language for data analysis and graphics. *J Comput Graph Stat* 5:299–314

Itahana K, Zou Y, Itahana Y, Martinez JL, Beausejour C, Jacobs JJ *et al.* (2003) Control of the replicative life span of human fibroblasts by p16 and the polycomb protein Bmi-1. *Mol Cell Biol* 23:389–401

Jacobs JJL, de Lange T (2004) Significant role for $p16^{INK4a}$ in p53-independent telomere-directed senescence. *Curr Biol* 14:2302–8

Karlseder J, Smogorzewska A, de Lange T (2002) Senescence induced by altered telomere state, not telomere loss. *Science* 295:2446–9

Kim NM, Piatyszek MA, Prowse KR, Harley CB, West MD, Ho PLC *et al.* (1994) Specific association of human telomerase activity with immortal cells and cancer. *Science* 266:2011–5

Kiyono T, Foster SA, Koop JI, McDougall JK, Galloway DA, Klingelhutz AJ (1998) Both Rb/p16INK4a inactivation and telomerase activity are required to immortalize human epithelial cells. *Nature* 396:84–8

Kraus J, Pantel K, Pinkel D, Albertson DG, Speicher MR (2003) High-resolution genomic profiling of occult micrometastatic tumor cells. *Genes Chromosomes Cancer* 36:159–66

Krishnamurthy J, Torrice C, Ramsey MR, Kovalev GI, Al-Regaiey K, Su L-K *et al.* (2004) Ink4a/Arf expression is a biomarker of aging. *J Clin Invest* 114:1299–307

Kurochkin IV, Yonemitsu N, Funahashi SI, Nomura H (2001) ALEX1, a novel human armadillo repeat protein that is expressed differentially in normal tissues and carcinomas. *Biochem Biophys Res Commun* 280: 340–7

Li S, Crothers J, Haqq CM, Blackburn EH (2005) Cellular and gene expression responses in the rapid growth inhibition of human cancer cells by RNA interference-mediated depletion of telomerase RNA. *J Biol Chem* 280: 23709–17

Lin S-Y, Elledge SJ (2003) Multiple tumor suppressor pathways negatively regulate telomerase. *Cell* 113:881–9

Maser RS, DePinho RA (2002) Connecting chromosomes, crisis and cancer. *Science* 297:565–9

Masutomi K, Yu EY, Khurts S, Ben-Porath I, Currier JL, Metz GB *et al.* (2004) Telomerase maintains telomere structure in normal human cells. *Cell* 114:241–53

Morales C, Holt SE, Ouellette M, Kaur KJ, Yan Y, Wilson KS *et al.* (1999) Absence of cancer-associated changes in human fibroblasts immortalized with telomerase. *Nat Genet* 21:115–8

Morin GB (1995) Is telomerase as universal cancer target? *J Nat Cancer Inst* 87:859–61

Piatyszek MA, Kim NW, Weinrich SL, Hiyama K, Hiyama E, Wright WE *et al.* (1995) Detection of telomerase activity in human cells and tumors by telomeric repeat amplification protocol (TRAP). *Methods Cell Sci* 17:1–5

Racek T, Mise N, Li Z, Stoll A, Putzer BM (2005) C-terminal p73 isoforms repress transcriptional activity of the humnan telomerase reverse transcriptase (hTERT) promoter. *J Biol Chem* 280:40402–5

Ray SS, Swanson HI (2004) Dioxin-induced immortalization of normal human keratinocytes and silencing of p53 and $p16^{INK4a}$. *J Biol Chem* 279: 27187–93

Rea MA, Gregg JP, Qin Q, Phillips MA, Rice RH (2003) Global alteration of gene expression in human keratinocytes by inorganic arsenic. *Carcinogenesis* 24:747–56

Rea MA, Phillips MA, deGraffenried LA, Qin Q, Rice RH (1998) Modulation of human epidermal cell response to 2, 3, 7, 8-tetrachlorodibenzo-p-dioxin by epidermal growth factor. *Carcinogenesis* 19:479–83

Rea MA, Rice RH (2000) Effect of TCDD on telomerase activity of spontaneously immortalized keratinocytes. *Organohalogen Compounds* 49:151–4

Rea MA, Rice RH (2001) Telomerase deregulation in immortalized human epidermal cells: modulation by cellular microenvironment. *Int J Cancer* 94:669–73

Rheinwald JG, Beckett MA (1981) Tumorigenic keratinocyte lines requiring anchorage and fibroblast support cultured from human squamous carcinomas. *Cancer Res* 41:1657–63

Rheinwald JG, Green H (1975) Serial cultivation of strains of human epidermal keratinocytes: the formation of keratinizing colonies from single cells. *Cell* 6:331–44

Rheinwald JG, Hahn WC, Ramsey MR, Wu JY, Guo Z, Tsao H *et al.* (2002) A two-stage, $p16^{INK4a}$- and p53-dependent keratinocyte senescence mechanism that limits replicative potential independent of telomere status. *Mol Cell Biol* 22:5157–72

Rice RH, Steinmann KE, deGraffenried LA, Qin Q, Taylor N, Schlegel R (1993) Elevation of cell cycle control proteins during spontaneous immortalization of human keratinocytes. *Mol Biol Cell* 4: 185–94

Romanov SR, Kozakiewicz BK, Holst CR, Stampfer MR, Haupt LM, Tlsty TD (2001) Normal human mammary epithelial cells spontaneously escape senescence and acquire genomic changes. *Nature* 409: 633–7

Rubin H (2002) The disparity between human cell senescence *in vitro* and lifelong replication *in vivo*. *Nat Biotech* 20:675–81

Rudolph KL, Chang S, Lee H-W, Blasco M, Gottlieb GJ, Greider CW *et al.* (1999) Longevity, stress response, and cancer in aging telomerase-deficient mice. *Cell* 96:701–12

Rudolph KL, Millard M, Bosenberg MW, DePinho RA (2001) Telomere dysfunction and evolution of intestinal carcinoma in mice and humans. *Nat Genet* 28:155–9

Shay JW, Wright WE (2000) The use of telomerized cells for tissue engineering. *Nat Biotech* 18:22–3

Sherr CJ, DePinho RA (2000) Cellular senescence: mitotic clock or culture shock? *Cell* 102:407–10

Shi S, Gronthos S, Chen S, Reddi A, Counter CM, Robey PG *et al.* (2002) Bone formation by human postnatal bone marrow stromal stem cells is enhanced by telomerase expression. *Nat Biotech* 20:587–91

Simonsen JL, Rosada C, Serakinci N, Justesen J, Stenderup K, Rattan SIS *et al.* (2002) Telomerase expression extends the proliferative life-span and maintains the osteogenic potential of human bone marrow stromal cells. *Nat Biotech* 20:592–6

van Heek NT, Meeker AK, Kern SE, Yeo CJ, Lillemoe KD, Cameron JL *et al.* (2002) Telomere shortening is nearly universal in pancreatic intraepithelial neoplasia. *Am J Pathol* 161:1541–7

Wege H, Chui MS, Le HT, Tran JM, Zern MA (2003) SYBR green real-time telomeric repeat amplification protocl for the rapid quantification of telomerase activity. *Nucleic Acids Res* 31:E3-3

Wright WE, Shay JW (2002) Historical claims and current interpretations of replicative aging. *Nat Biotech* 20:682–8

Yang J, Nakavarapu U, Relloma K, Sjaastad MD, Moss WC, Passaniti A *et al.* (2001) Telomerized human microvasculature is functional *in vivo*. *Nat Biotech* 19:219–24